

Open Research Online

The Open University's repository of research publications and other research outputs

A CMOS TDI image sensor for Earth observation

Conference or Workshop Item

How to cite:

Rushton, Joseph E.; Stefanov, Konstantin D.; Holland, Andrew D.; Endicott, James; Mayer, Frederic and Barbier, Frederic (2015). A CMOS TDI image sensor for Earth observation. In: Proceedings of SPIE, SPIE, 9616.

For guidance on citations see [FAQs](#).

© 2015 Society of Photo-Optical Instrumentation Engineers (SPIE).

Version: Accepted Manuscript

Link(s) to article on publisher's website:
<http://dx.doi.org/doi:10.1117/12.2187952>

Copyright and Moral Rights for the articles on this site are retained by the individual authors and/or other copyright owners. For more information on Open Research Online's data [policy](#) on reuse of materials please consult the policies page.

oro.open.ac.uk

A CMOS TDI image sensor for Earth observation

Joseph E. Rushton^a, Konstantin D. Stefanov^a, Andrew D. Holland^a, James Endicott^b.

^aCentre For Electronic Imaging, The Open University, MK7 6AA, UK;

^be2v technologies, Waterhouse Lane, Chelmsford, CM1 2QU, UK

ABSTRACT

Time Delay and Integration (TDI) is used to increase the Signal to Noise Ratio (SNR) in image sensors when imaging fast moving objects. One important TDI application is in Earth observation from space. In order to operate in the space radiation environment, the effect that radiation damage has on the performance of the image sensors must be understood.

This work looks at prototype TDI sensor pixel designs, produced by e2v technologies. The sensor is a CCD-like charge transfer device, allowing in-pixel charge summation, produced on a CMOS process. The use of a CMOS process allows potential advantages such as lower power consumption, smaller pixels, higher line rate and extra on-chip functionality which can simplify system design. CMOS also allows a dedicated output amplifier per column allowing fewer charge transfers and helping to facilitate higher line rates than CCDs.

In this work the effect on the pixels of radiation damage from high energy protons, at doses relevant to a low Earth orbit mission, is presented. This includes the resulting changes in Charge Transfer inefficiency (CTI) and dark signal.

1. INTRODUCTION

TDI mode imaging allows an increase in signal to noise ratio when imaging a moving scene. One way this can be achieved is by transferring the accumulated photo generated charge across an imaging array so that it tracks the moving illumination of the array by the scene thus increasing the effective exposure time. CCDs are inherently suited to TDI mode imaging as charge transfer is integral to their operation. Applications include industrial process monitoring and Earth observation from aircraft or spacecraft.

CMOS Image Sensors (CIS) are also able to perform TDI mode imaging by summing the output from many frames with the necessary translation, equivalent to summing the output from multiple line-scan cameras. This has the disadvantage of increasing read noise with every additional line. CCD TDI imaging only requires the charge measurement once for each element of the image, despite the element having been accumulated from many pixels in turn.

There are, however, advantages to the use of modern CMOS process when manufacturing sensors: lower power consumption, extra on chip systems (clock drivers, ADCs, signal processing), lower pixel sizes, lower cost etc. CMOS sensors are also widely considered to be radiation hard.

The main challenge to using modern CMOS processes tailored for APS for CCD style image sensors is that the Charge Transfer Inefficiency (CTI) must be kept low and this is difficult without considerable process optimisation. In TDI mode this requirement is relaxed as parallel register CTI does not limit the image pixel count achievable, only the number of SNR enhancing stages.

*E-mail: joseph.rushton@open.ac.uk

The CTI has improved considerably over the first prototype^{1,2} which means that a more refined method is now needed to accurately measure CTI. In this work we start with a review of the Toad 2 chip and the EPER technique for CTI measurement. Then we discuss some of the challenges faced in trying to measure CTI in this device and present our results for CTI in the different pixel variants and at different pixel clock voltages. Finally we present the results of a proton radiation campaign on two test devices at fluences relevant to a low earth orbit mission.

2. TOAD 2 TDI CMOS TEST CHIP

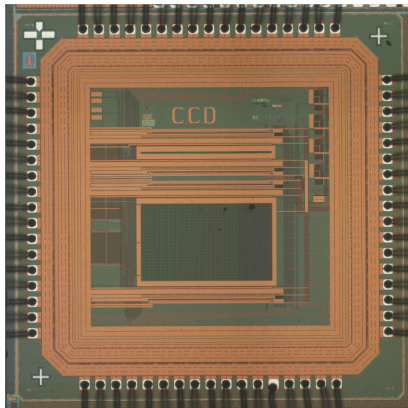


Figure 1. A photograph of the TDI CMOS test chip. The central area is the pixel array and the transfer direction is down the page.

The Toad 2 prototype (Figure 1) is a TDI mode CCD-like image sensor chip designed by e2v technologies.³ The chip uses $13\mu\text{m}$ pixels and is built on a $0.18\mu\text{m}$ CMOS image sensor process. The test chip has 40 rows (TDI stages) and 8 blocks of different pixel designs, each block with 8 columns making a 40×64 pixel array. The pixel full well capacity is in the region of 110ke^- with Anti-Blooming (AB) disabled and the devices operating from a 5 V supply.

The four phase buried channel CCD-like architecture (figure 3) has a CCD style output with reset level followed by signal level. There is an output amplifier at both ends (top and bottom) of every column and two top outputs and two bottom outputs are available for measurement at once. The measurement circuitry (figure 2) also doubles as a charge injection structure. A summary of the different pixel variants studied in this work are shown in table 1.

Block no.	0	1	2	3	4	5
AB gate	Buried	Buried	Buried	Surface	Surface	Surface
Interpoly gap (μm)	0.2	0.25	0.25	0.25	0.25	0.2
Implant split	A	A	B	C	D	D

Table 1. Summary of the design choices for the six pixel designs studied in this work.

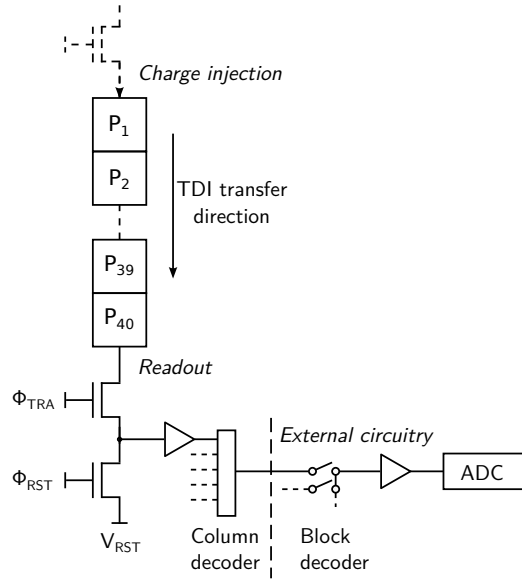


Figure 2. Each 40 pixel column has dedicated readout electronics leading to an on-chip column decoder. An identical structure is present at the top of the column which serves as a charge injection mechanism.

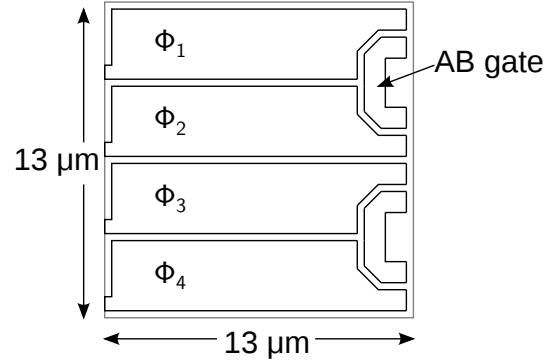


Figure 3. The four-phase CCD-like pixel architecture showing the transfer and antiblooming gate arrangements.

3. CTI MEASUREMENT

3.1 Extended pixel edge response

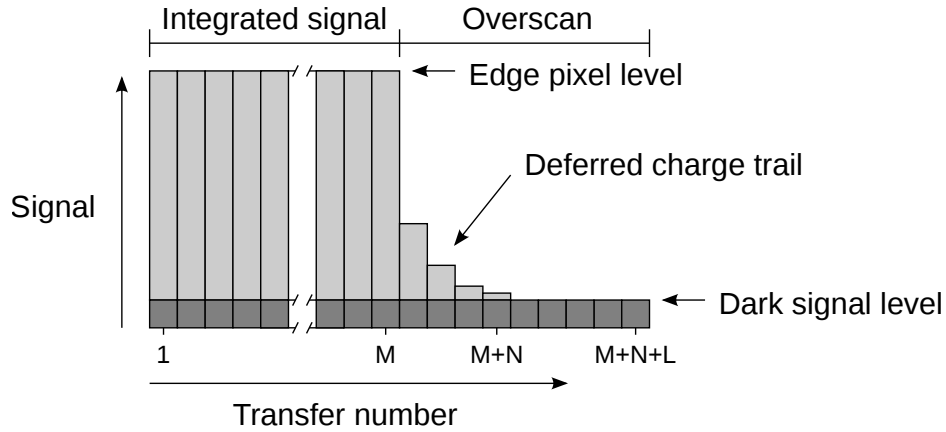


Figure 4. CTI can be measured by EPER using the dark current collected after an integration period. The dark signal collected during readout and any offset is also measured and subtracted from the pixel edge level and the deferred charge trail.

The methods chosen to measure CTI was the Extended Pixel Edge Response (EPER)⁴ by charge injection and dark current (figure 4). Alternatives, such as the use of ⁵⁵Fe X-rays, were considered. This would require a

very large flux to acquire useful statistics, given the small pixel count in the device, and would provide essentially only one signal level. By contrast, the use of either dark current or injected charge allows a user-selected signal count to occur in every frame.

The EPER method involves first filling a pixel with a charge packet of a certain size (E) and then removing the charge by transferring it into an adjacent pixel or the output node. The “edge” refers to the contrast between the pixel containing the charge packet and the following pixel, which ideally only contains a small dark signal. Most of the charge, $\alpha \cdot S$, will be removed on the first transfer and subsequent transfers will drive out the small residual charge $\epsilon \cdot E$, which has been trapped. The residual charge can be observed on the output of the device in the form of a charge trail. If a charge packet E is present in the last pixel of the column, after one transfer the charge measured at the output will be

$$n[1] = \alpha \cdot E + n_{ds} \quad (1)$$

and the deferred charge can be found from

$$\epsilon \cdot E = \sum_{i=2}^{\infty} (n[i] - n_{ds}) \quad (2)$$

where $n[i]$ is the charge measured at the output after i transfers and n_{ds} is the charge due to dark signal in the overscan. In our experiment we are unable to directly place charge into only the last pixel. Our choices are to inject charge into the first pixel or integrate dark signal in all pixels. Since the edge pixels (first and last in the column) have partial shielding this precludes us from using flat field optical generation as the brighter middle pixels immediately precede the dimmer edge pixel. This means that the pixel edge appears at the output after M transfers, where $M = 40$ is the number of pixels in a column. We assume that $\alpha \approx 1$ such that the pixel edge is a good approximation of the original signal E even though some charge has been lost to traps. If M is sufficiently large an equilibrium will be reached between trap capture and emission which makes this approximation even better. Therefore we can generalise that

$$E = n[M] - n_{ds} \quad (3)$$

$$\sum_{i=M+1}^{\infty} (n[i] - n_{ds}) = M \cdot \epsilon \cdot E \quad (4)$$

and use this to measure the CTI, ϵ .

Using a finite length frame we can approximate the charge trail magnitude as

$$M \cdot \epsilon \cdot E = \sum_{i=M+1}^{M+N} (n[i] - n_{ds}) \quad (5)$$

where N is the number of transfers required for the charge trail to become invisible above the noise floor. An estimate for n_{ds} is easily computed in the same frame using the mean

$$\overline{n_{ds}} = \frac{1}{L} \sum_{i=M+N+1}^{M+N+L} n[i] \quad (6)$$

where $M + N + L$ is the total frame length.

We have assumed that the charge trail is not sensitive to the number of injections. This assumption is made given that any trap capture time constant τ_c is likely to be very short compared to the time which the signal spends in the vicinity of any particular trap. The assumption can only be valid if the preceding charge packets were smaller than, or equal in size to, the edge packet, E . Larger packets would leave charge trails of their own which would appear on top of the desired signal. We also require the Dark Signal Non Uniformity (DSNU) down the column to be sufficiently small or for the order of brighter and darker pixels to be conducive to a sharp edge.

3.2 Actual EPER trails

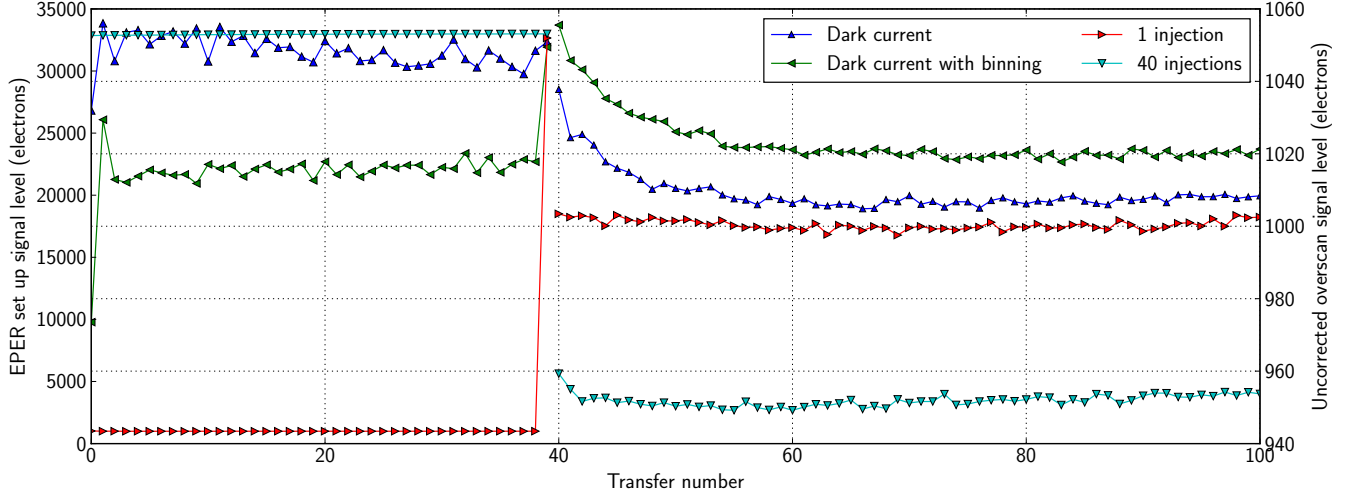


Figure 5. The edge pixel charge packet can be generated by dark current or charge injection. In each case, for a particular charge packet size (33 ke^- shown here) the ensuing charge trails (magnified scale after transfer number 40) have different magnitudes. Additionally, the charge trails decay to different time-varying levels.

Figure 5 shows actual charge trails for edges generated by dark current, dark current binning, and charge injection for 1 and 40 transfers. In each case the edge charge packet is of approximately equal size at 33 ke^- . The dark current binning is achieved by holding all four clock phases high during integration with the aim of reducing the effect of DSNU. In fact the result is that charge accumulates preferentially in the first and last pixel.

The actual trails present two problems: Firstly, the trail of deferred charge visible in each case does not decay to a constant signal level. This is a problem as subtraction of dark current and offset becomes difficult. Further investigation has shown that the underlying overscan signal is a function of integrated or injected signal level and timing and also a function of the length of overscan. This suggests that it is an electrical filtering effect of some kind not necessarily intrinsic to the device itself. The exact cause remains unknown and the effect is subtle with the distortion is in the region of $100\text{ }\mu\text{V}$.

Secondly, figure 5 also shows that the magnitude of the charge trail is not consistent between the dark current generation and charge injection methods. It is also affected by the number of injections. This suggests that our assumptions about immediate electron capture may be naïve and we suspect that dwell time may have a strong effect on the number of trapped electrons. This is an ongoing area of investigation.

3.3 Absolute CTI estimation

In order to make an absolute measurement of the deferred charge and consequently the CTI it is necessary to recover the charge trail from the underlying overscan waveform. Our general method for doing so is to first choose the charge trail length N . Having done this we choose a length of waveform immediately following the charge trail, of length L , to which we fit a function. We then extrapolate the fitted function backwards as our estimate of dark signal and offset. The estimate for deferred charge is obtained by subtracting the extrapolated fit from the charge trail and integrating.

In order to choose N and L we need to find a way to distinguish between the charge trail and the underlying waveform. Some proposed methods for doing this automatically are as follows:

One approach has been to model the deferred charge signal as a decaying exponential of the form $f[p] = Ae^{-p/\tau_f}$ based on simple Shockley-Read-Hall trap release model.⁵ By fitting a function $f[p] = Ae^{-p/\tau_f} + Bx + C$ we obtain a coarse estimate for the time constant τ_f .

Another option is to smooth the data and then choose a threshold on the second derivative. The threshold is chosen at the point where the fast changing exponential no longer dominates over the more slowly evolving underlying function. This method is very sensitive to the smoothing algorithm used. In both cases we find $N \approx 20$ to be an appropriate estimate.

Figure 6 shows the deferred charge measurement against signal for $N=10, 20, 30$ and $L=10$. Clearly the measurement is sensitive to N but the two regimes are clearly visible. Below $\approx 60 \text{ ke}^-$ the deferred charge is low and above this signal level it rises rapidly, presumably due to charge hitting the surface.

Figure 7 demonstrates the cause of some of the large variation in measurement as the overscan shape changes with edge signal size. Also shown is the corrected charge trail after fitting and subtraction.

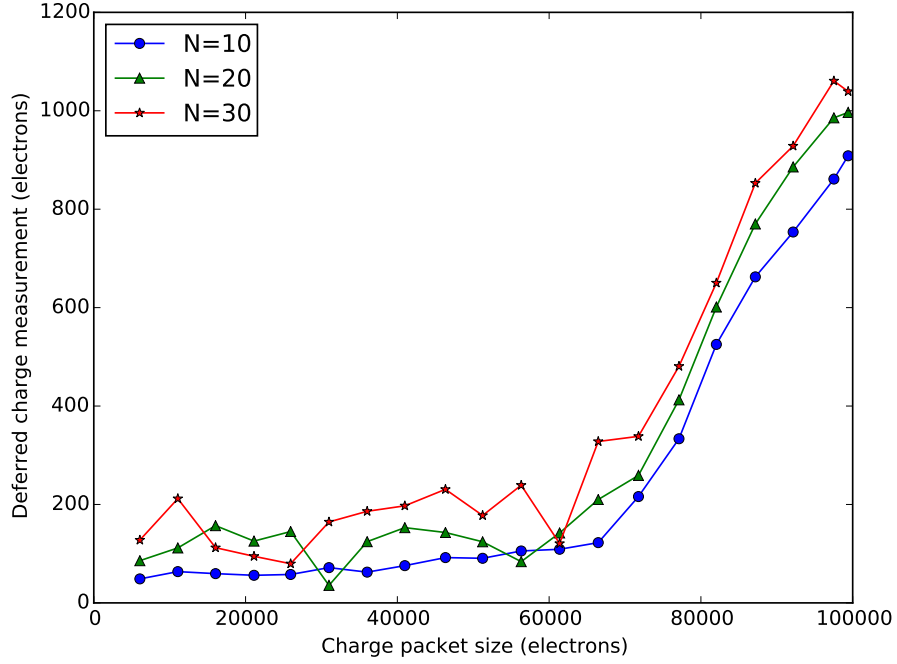


Figure 6. The deferred charge measured as by EPER has two regimes. The sharp rise is assumed to be from carriers hitting the surface. Calculation from a short length of overscan (low N) underestimates the deferred charge and therefore the CTI whereas a high N introduces large errors due to difficulty fitting to the overscan.

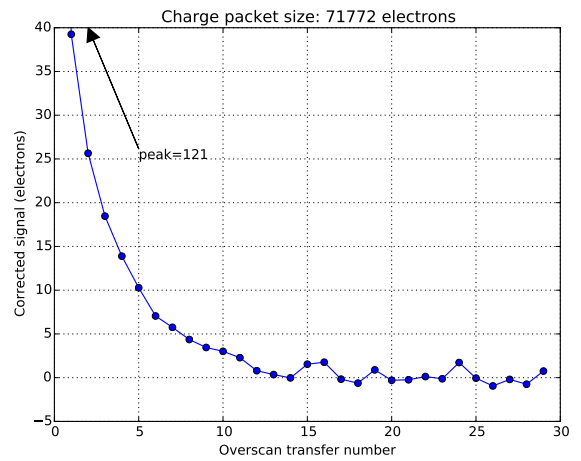
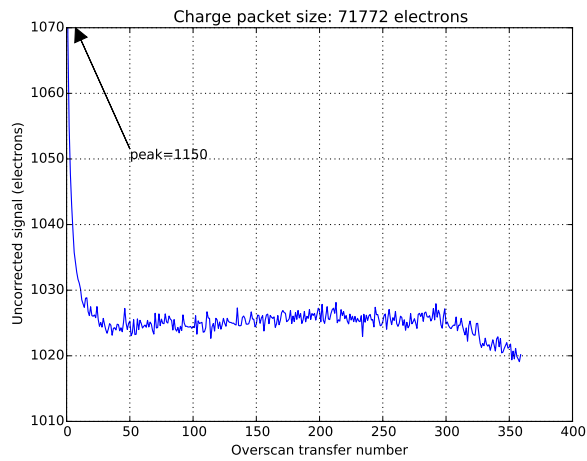
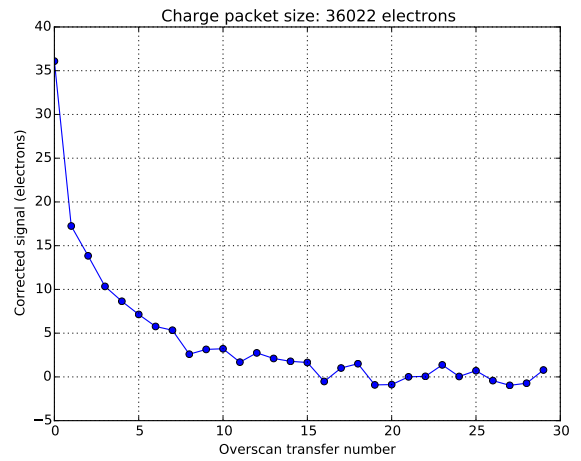
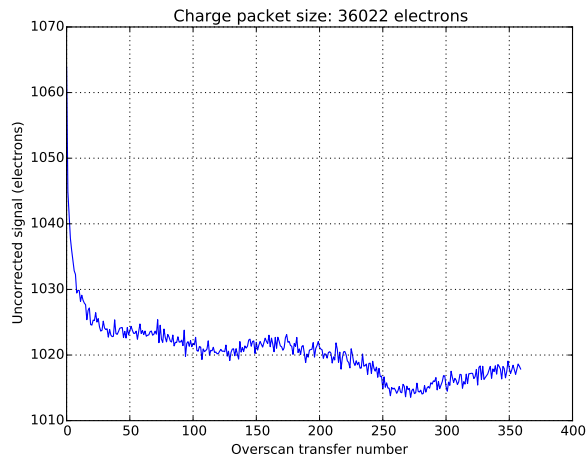
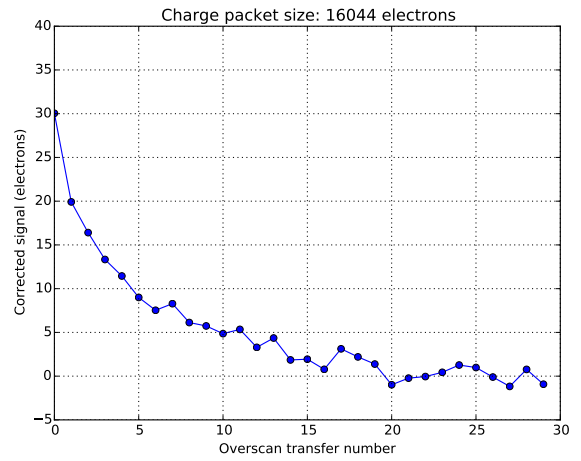
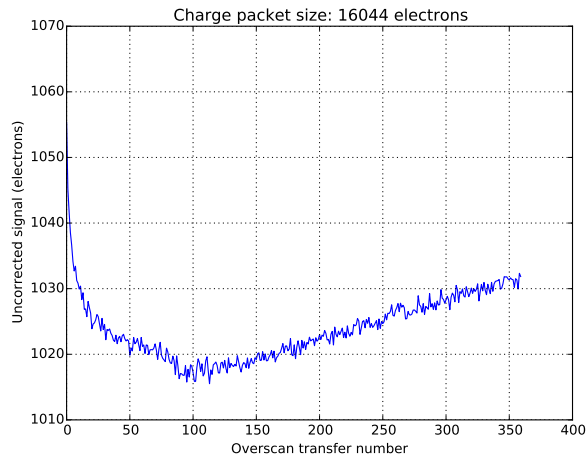


Figure 7. A selection of “awkward” frames to be analysed (left) and the corrected charge trails using $N=20$ and $L=10$ (right).

3.4 Design and operation effects on CTI

The CTI was measured using dark current at 25 °C with the device running at a pixel rate of 12.5 kHz (at least 50 kHz is possible) and using $N=20$ and $L=10$. The chip temperature was maintained with a thermo-electric cooler and measured with a platinum resistance thermometer fixed to the chip. CTI was averaged across columns in the same design block.

Figure 8 shows the CTI measured against signal level for 6 of the different pixel designs on the chip referred to in table 1. The full well capacities show some variation but the mid signal CTI is similar across designs at $< 2 \times 10^{-4}$. Block 2 has the lowest CTI but also the lowest full well capacity.

Figure 9 shows how CTI is affected by a change of clock voltage $V\phi$ for design block 0. At higher clock voltages the onset of the surface trap related CTI increase happens at lower signal levels.

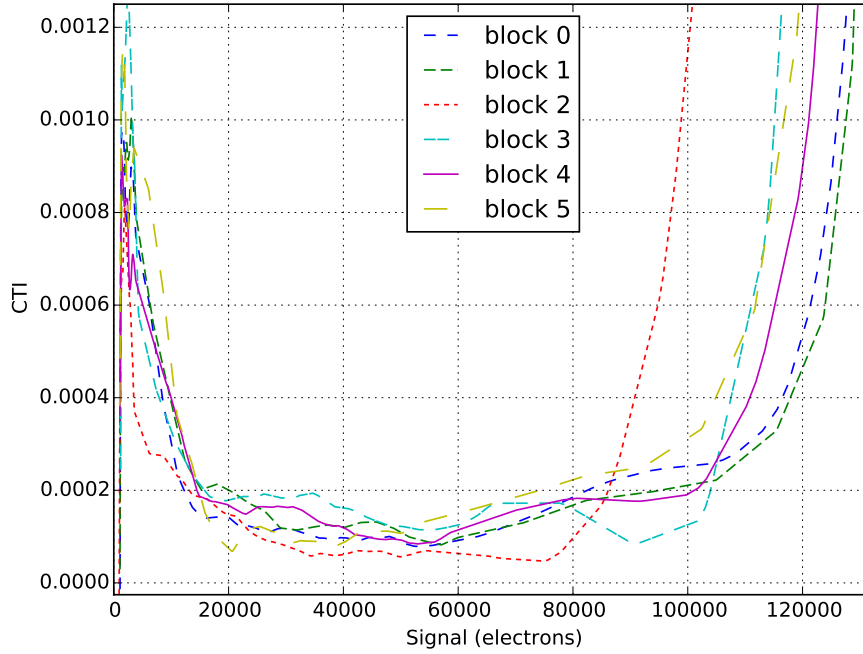


Figure 8. The mid-signal CTI in all pixel design blocks is $< 2 \times 10^{-4}$. Block 2 has the lowest CTI but also the lowest full well capacity.

4. RADIATION DAMAGE EFFECTS

In order to start to an assessment the suitability of the Toad 2 sensor for use in low earth orbit applications two test devices were irradiated with 74 MeV protons at the Paul Scherrer Institut in Switzerland. The 10 MeV equivalent fluences used were $5 \times 10^9 \text{ cm}^{-2}$ and $1 \times 10^{10} \text{ cm}^{-2}$.

4.1 CTI increase

The CTI increase at both fluences was undetectable above the errors in fitting to the overscan (figure 10). The repeatability of our CTI measurements is good, but the increased dark current from radiation damage means that the output signal timing and amplitude change from pre- to post-irradiation. In other words, because a particular edge pixel signal level is reached more quickly with higher dark current, the overscan waveform is altered at that signal level by the irradiation.

To produce a measurable CTI increase we are arranging for a further irradiation up to 10 MeV equivalent fluences of $5 \times 10^{10} \text{ cm}^{-2}$ and $1 \times 10^{11} \text{ cm}^{-2}$ (making the fluences larger by a factor of 10).

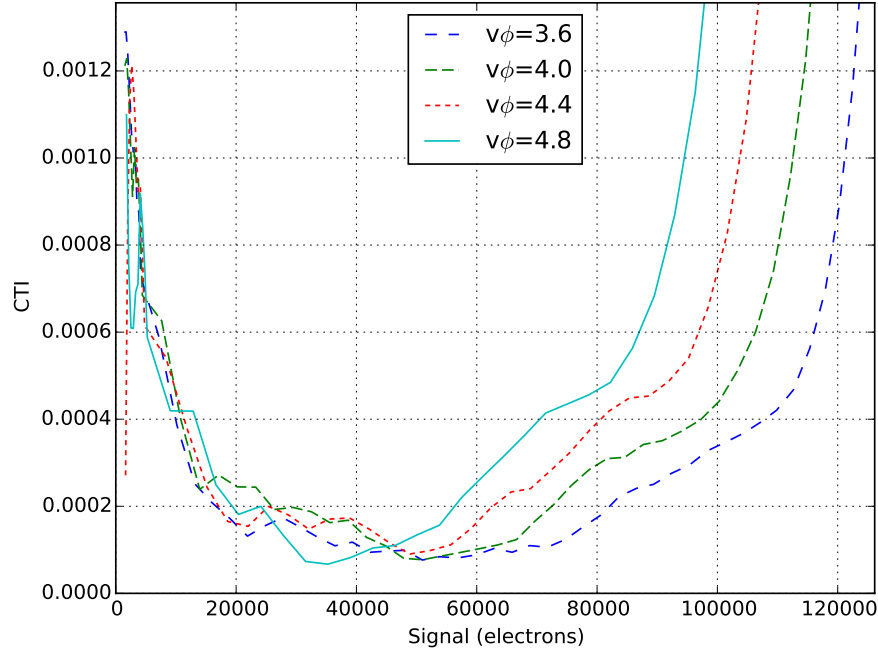


Figure 9. A reduced clock voltage $V\phi$ has the effect of increasing full well capacity. Results from pixel design block 0 are shown.

4.2 Dark current increase

The average dark current at 25 °C was measured before irradiation at around 20 nA cm^{-2} and increased by 10-15% with the $1 \times 10^{10} \text{ cm}^{-2}$ 10 MeV equivalent proton damage (figure 11). In some design blocks the DSNU is large before the irradiation and this seems to be a processing effect. In all design blocks, except block 0, the proportional dark current increase was greater at the higher fluence (figure 12).

5. CONCLUSIONS AND FURTHER WORK

The Toad 2 TDI CMOS image sensor shows promising performance for use in space applications. We have estimated the mid signal CTI is below 2×10^{-4} and the sensor requires a small number of transfers. In addition, exposure to high energy protons at 10 MeV equivalent fluences of $5 \times 10^9 \text{ cm}^{-2}$ and $1 \times 10^{10} \text{ cm}^{-2}$ has so far shown only a small effect on CTI which is a good result for use in space environments. The dark current increase at these fluences is only moderate.

We have discussed some of the challenges in making an accurate estimate of the CTI using EPER. Further work will concentrate on refining our methods. The dependence of CTI on charge dwell time in the pixels will also be investigated with the aim of understanding the discrepancies between the dark current and charge injection EPER methods.

Furthermore, we will be repeating the radiation damage work with 10 times the fluence of high energy protons.

REFERENCES

- [1] F. Mayer, H. Bugnet, S. Pesenti, C. Guicherd, B. Gili, R. Bell, B. De Monte, and T. Ligozat, "First measurements of true charge transfer TDI (time delay integration) using a standard CMOS technology,"
- [2] J. Rushton, A. Holland, K. Stefanov, and F. Mayer, "Characterisation of a CMOS charge transfer device for TDI imaging," *Journal of Instrumentation* **10**(03), p. C03027, 2015.

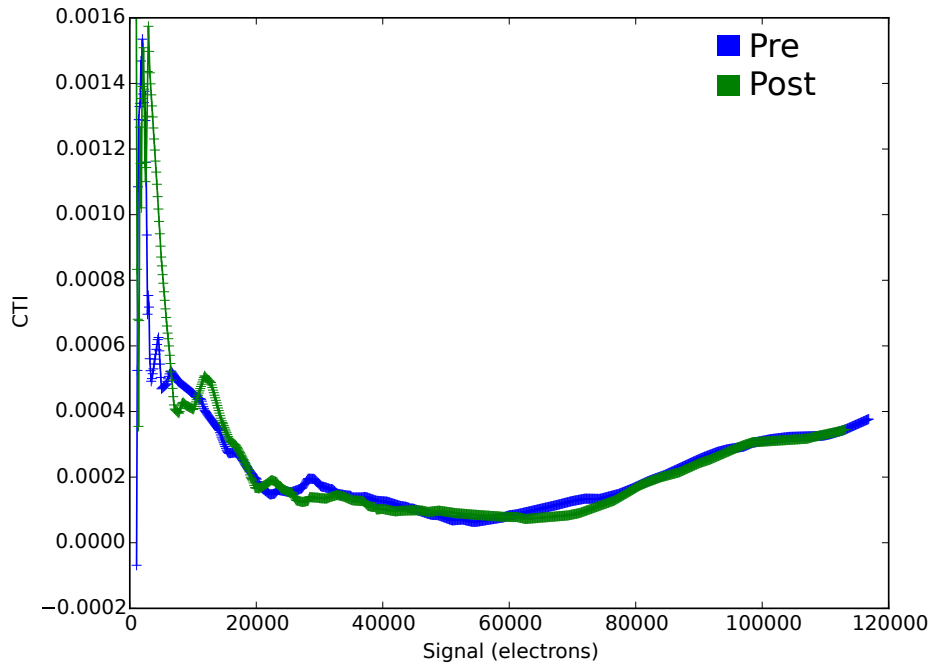


Figure 10. Any increase in CTI after irradiation with $1 \times 10^{10} \text{ cm}^{-2}$ 10 MeV equivalent protons is not visible above the errors introduced by the overscan fitting.

- [3] F. Mayer, S. Pesenti, F. Barbier, H. Bugnet, J. Endicott, F. Devriere, and T. Ligozat, “CMOS charge transfer TDI with front side enhanced quantum efficiency,”
- [4] J. R. Janesick, *Scientific charge-coupled devices*, SPIE press Bellingham, 2001.
- [5] S. Sze, *Physics of semiconductor devices*, Wiley-Interscience, New York, NY, 1981.

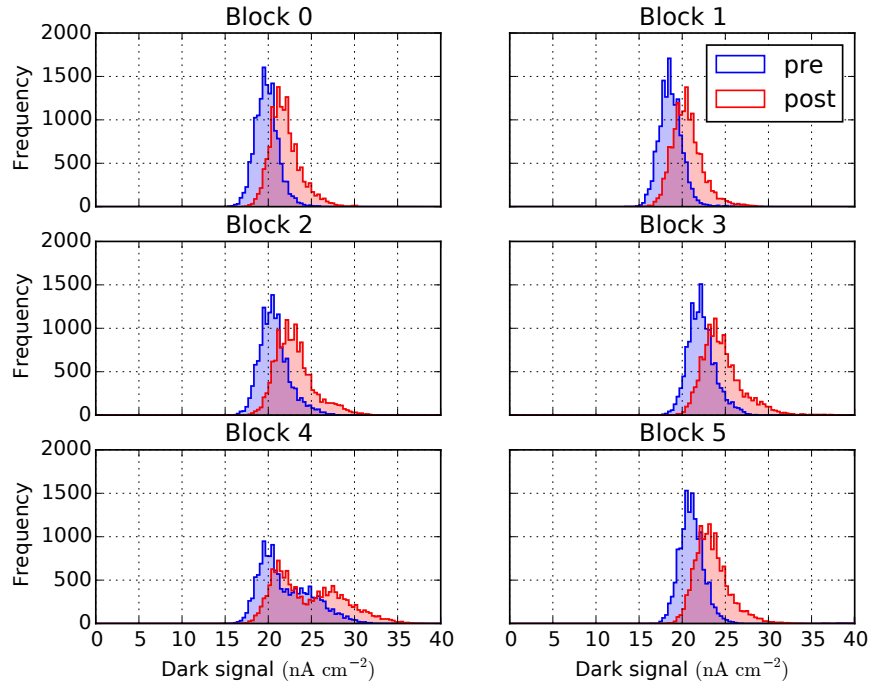


Figure 11. After a $1 \times 10^{10} \text{ cm}^{-2}$ fluence of 10 MeV equivalent protons the dark current increased by approximately 10 - 15%.

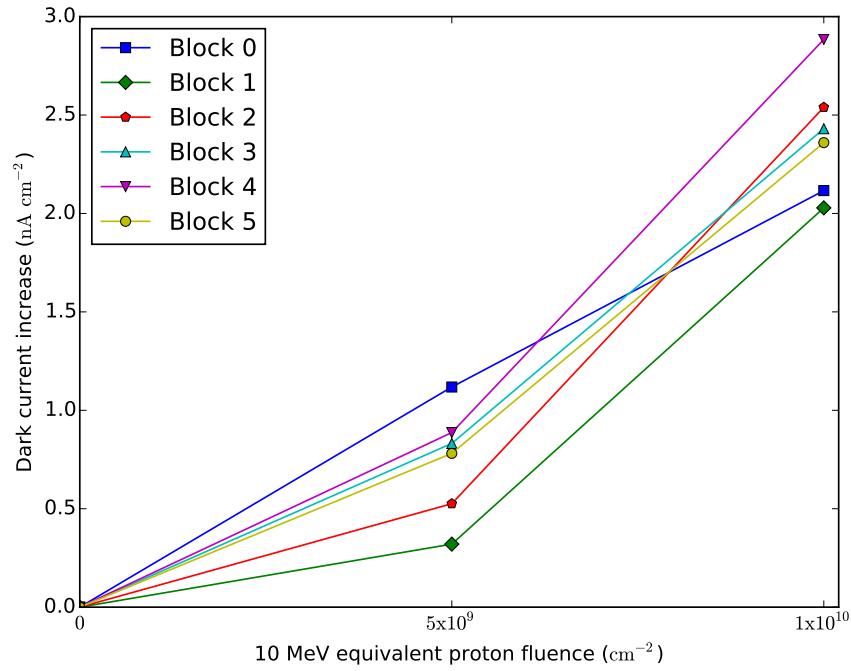


Figure 12. In all but one pixel design block, the proton irradiation dark current increase per fluence seems to be greater after the higher ($1 \times 10^{10} \text{ cm}^{-2}$ 10 MeV equivalent) fluence.